

## Supplementary Information

for

### **Vapochromic luminescence of a spin-coated copper(I) complex thin film by the direct coordination of vapour molecules**

*Sae Kondo, Nobutaka Yoshimura, Masaki Yoshida, Atsushi Kobayashi, Masako Kato*

*Department of Chemistry, Faculty of Science, Hokkaido University, North 10 West 8, Kita-ku, Sapporo, Hokkaido  
060-0810*

## Contents

**Fig. S1** Emission decays of **Cu-py@PVP** (blue) and **Cu-py crystal** (black) (at 298 K,  $\lambda_{\text{ex}} = 337$  nm).

**Fig. S2** Changes of emission spectra ( $\lambda_{\text{ex}} = 350$  nm) of (a) **Cu-Mepyz** and (b) **Cu-py** under exposure to py and Mepyz vapour, respectively at 298 K.

**Fig. S3** (a) Emission spectra of **Cu-Mepyz** (solid,  $\lambda_{\text{ex}} = 350$  nm) and (b) emission decays of **Cu-Mepyz** (solid,  $\lambda_{\text{ex}} = 337$  nm) at 298 K (red) and 77 K (blue).

**Fig. S4** Temperature-dependence of the emission lifetime of **Cu-Mepyz** in the solid state ( $\lambda_{\text{ex}} = 337$  nm).

**Fig. S5**  $^1\text{H}$  NMR spectrum of **Cu-Mepyz** crystal (400 MHz,  $\text{C}_2\text{D}_2\text{Cl}_4$ , 293 K).

**Fig. S6** Molecular structures of (a) **Cu-Mepyz** and (b) **Cu-py** with thermal vibrational ellipsoids at the 50% probability level.

**Fig. S7** Changes of PXRD patterns of **Cu-Mepyz** and **Cu-py** under exposure to py and Mepyz vapour respectively at 298 K.

**Fig. S8** Changes of  $^1\text{H}$  NMR spectrum in (a) aromatic region and (b) whole range of **Cu-py@PVP** before (blue) and after (red) exposure to Mepyz vapour (293 K, 400 MHz, in  $\text{C}_2\text{D}_2\text{Cl}_4$ ).

**Fig. S9** AFM images (top) and the height profile (bottom) of the surface of (A) the boundary area scratched **Cu-py@PVP** after exposure to Mepyz vapour and (B) Enlarged surface of **Cu-py@PVP** after exposure to Mepyz vapour.

**Fig. S10** Change of Chromaticity color coordinate plots for **Cu-py@PVP** (blue circle) after exposure to Mepyz vapour (red square) and the subsequent exposure to py vapour (black square).

**Fig. S11** Changes of emission spectra of **Cu-py@PVP** (blue lines) before and (red lines) after exposure to (a) pyrazine and (b) 2-methoxypyrazine vapour for 2 min (298 K,  $\lambda_{\text{ex}} = 350$  nm).

**Fig. S12** Photographs showing the luminescence changes for (a) **Cu-py** crystal and (b) **Cu-py@PVP** under exposure to Mepyz vapour. The right-side image in (a) is the photograph of crushed crystals after exposure to Mepyz vapour.

**Fig. S13** Changes of emission spectra ( $\lambda_{\text{ex}} = 350$  nm) at several different positions on **Cu-py@PVP** (blue lines) after exposure to Mepyz vapour (red line) and the subsequent exposure to py vapour (black dash line).

**Fig. S14** Schematic images of the experimental setup for (a) *in-situ* emission spectral measurement under vapour exposure and (b) *ex-situ* measurement for the vapour-exposed sample.

**Table S1** Crystal parameters and refinement data of **Cu-Mepyz** compared with **Cu-py**.

**Table S2** Selected bond lengths (Å) and angles (°) of **Cu-Mepyz** compared with **Cu-py**.

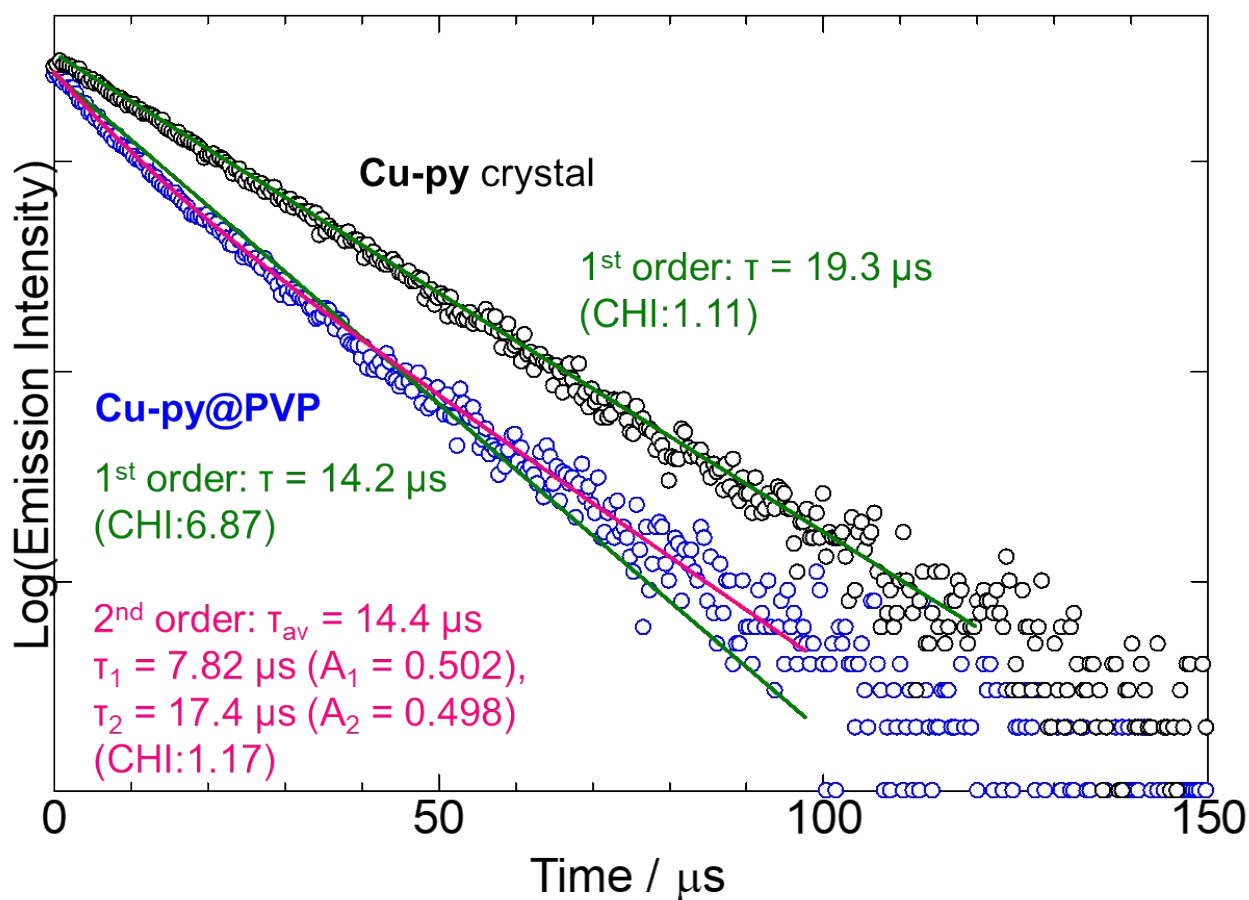


**Fig. S1** Emission decays of **Cu-py@PVP** (blue) and **Cu-py crystal** (black) (at 298 K,  $\lambda_{\text{ex}} = 337 \text{ nm}$ ).

Green and pink lines show the 1<sup>st</sup> and 2<sup>nd</sup> order fitting curves, respectively.

The 2<sup>nd</sup> order fitting:  $I = A_1 \exp(-t/\tau_1) + A_2 \exp(-t/\tau_2)$ . CHI = value of the  $\chi^2$  test.

The average emission lifetime:  $\tau_{\text{av}} = \sum A_i \tau_i^2 / \sum A_i \tau_i$  ( $i = 1, 2$ ).

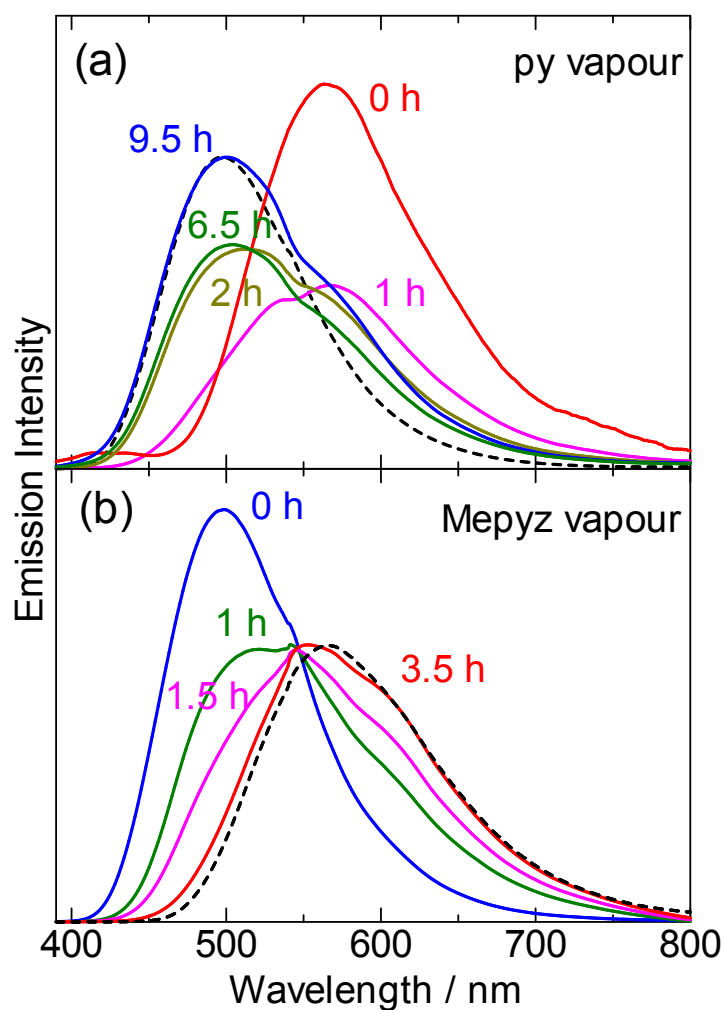


**Fig. S2** Changes of emission spectra ( $\lambda_{\text{ex}} = 350$  nm) of (a) **Cu-Mepyz** and (b) **Cu-py** on exposure to py and Mepyz vapour, respectively at 298 K. Each black dashed line in both panels shows the emission spectrum of (a) **Cu-py** and (b) **Cu-Mepyz**.

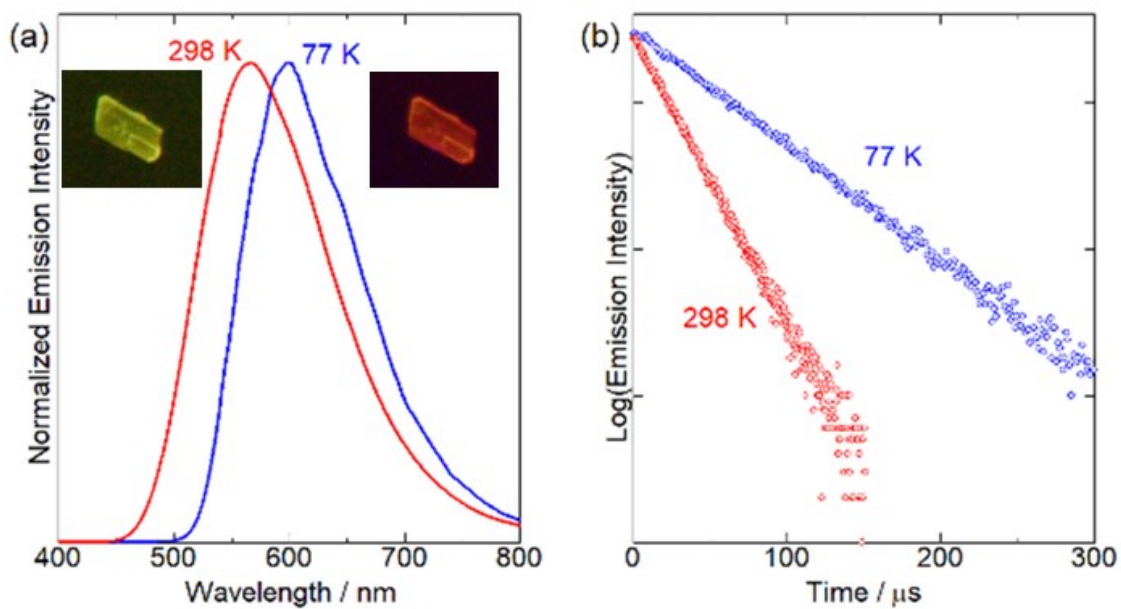


**Fig. S3** (a) Emission spectra of **Cu-Mepyz** (solid,  $\lambda_{\text{ex}} = 350$  nm) and (b) emission decays of **Cu-Mepyz** (solid,  $\lambda_{\text{ex}} = 337$  nm) at 298 K (red) and 77 K (blue). Inset in (a) is the photos of **Cu-Mepyz** under UV light irradiation. Photophysical Data at 298 and 77 K:  $\lambda_{\text{max}} = 566, 598$  nm;  $\tau = 22.5, 55.4$   $\mu\text{s}$ ;  $\Phi = 0.94, 0.77$ . The numerical data at 298 K are also included in Table 1.

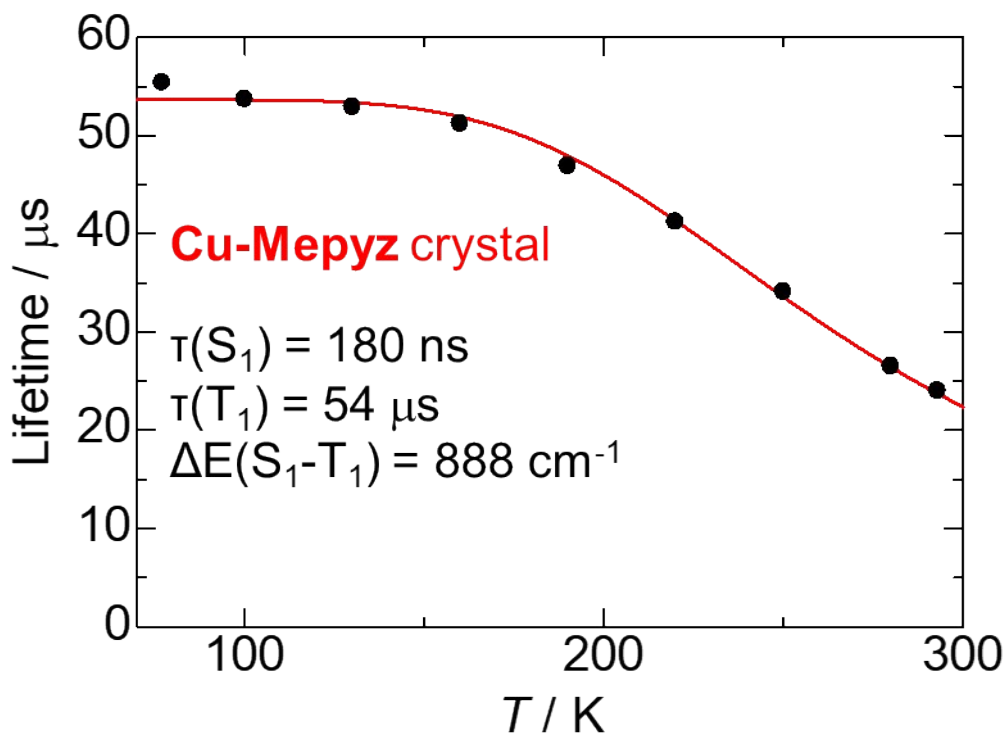


**Fig. S4** Temperature dependence of the emission lifetime of **Cu-Mepyz** in the solid state ( $\lambda_{\text{ex}} = 337$  nm). The red line is a calculated one from eq 1 based on the two-state ( $S_1$  and  $T_1$ ) model,<sup>S1</sup>

$$\tau(T) = \frac{3 + \exp\left[-\frac{\Delta E}{RT}\right]}{\frac{3}{\tau(T_1)} + \frac{1}{\tau(S_1)} \exp\left[-\frac{\Delta E}{RT}\right]} \quad (\text{eq 1})$$

where  $\Delta E$  is the energy difference between the singlet ( $S_1$ ) and triplet ( $T_1$ ) states,  $\tau(S_1)$  and  $\tau(T_1)$  are the lifetimes of the  $S_1$  (fluorescence) and  $T_1$  (phosphorescence) states,  $R$  is the ideal gas constant, and  $T$  is the absolute temperature.

---

S1. (a) M. J. Leitl, F. -R. K uchle, H. M. Mayer, L. Wesemann and H. Yersin, *J. Phys. Chem. A*, 2013, **117**, 11823–11826. (b) H. Ohara, A. Kobayashi and M. Kato, *Dalton Trans.*, 2014, **43**, 17317–17323.

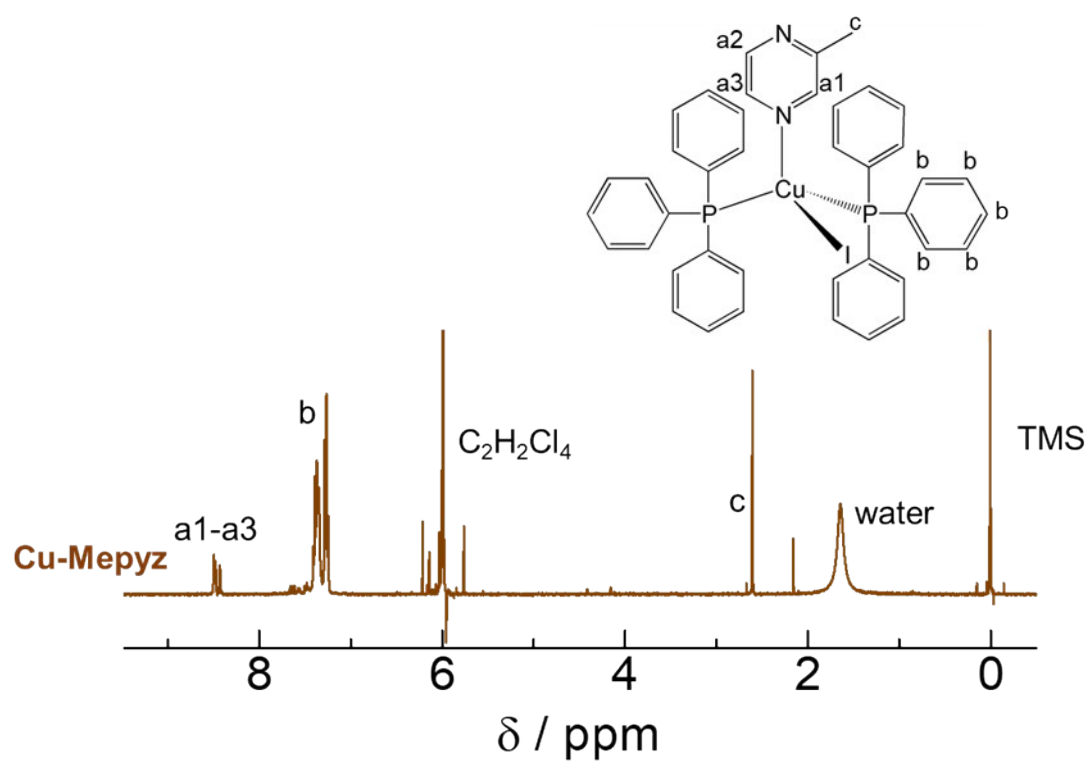


**Fig. S5**  $^1\text{H}$  NMR spectrum of the **Cu-Mepyz** crystal (400 MHz,  $\text{C}_2\text{D}_2\text{Cl}_4$ , 293 K).

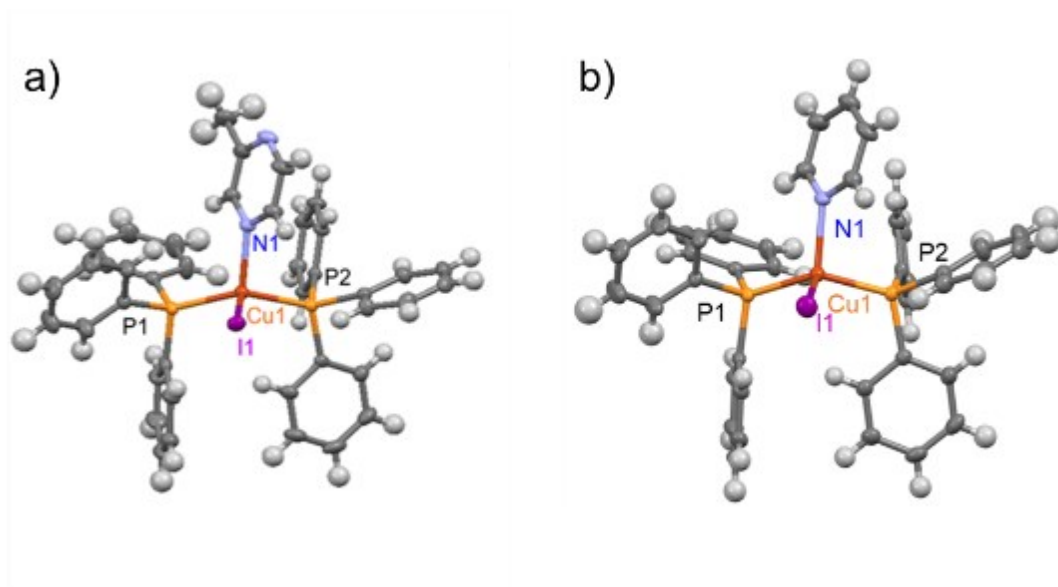


**Fig. S6** Molecular structures of (a) **Cu-Mepyz** and (b) **Cu-py** with thermal vibrational ellipsoids at the 50% probability level.



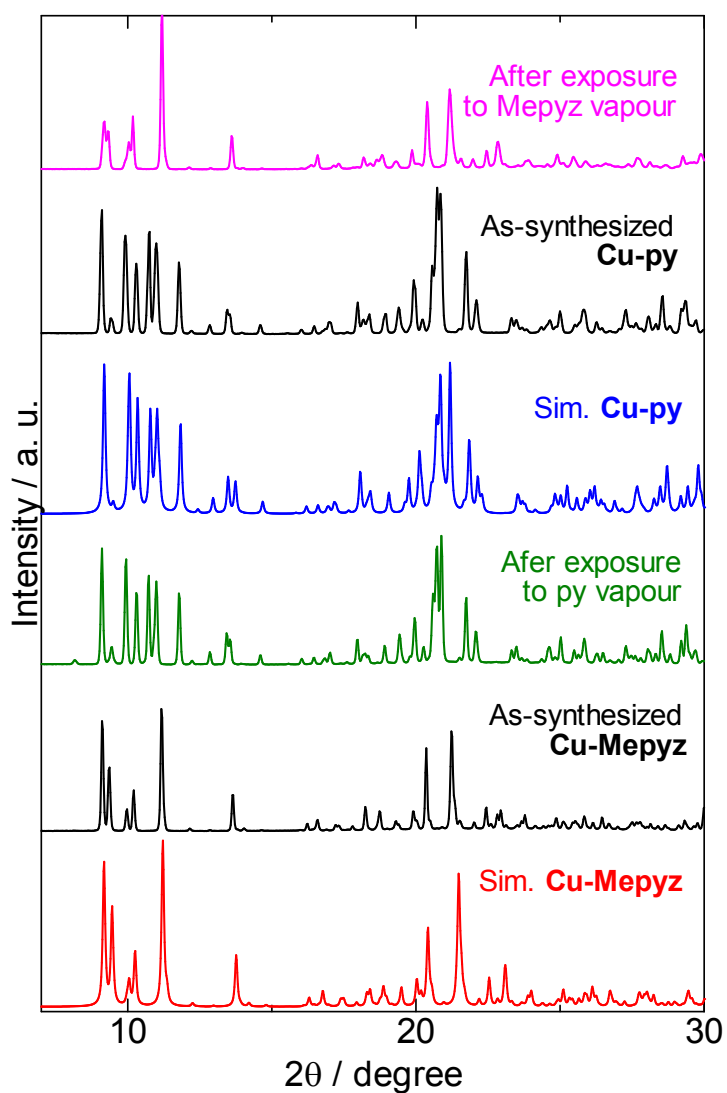


**Fig. S7** Changes of PXRD patterns of **Cu-Mepyz** and **Cu-py** under exposure to py and Mepyz vapour respectively at 298 K. Red and blue lines are the simulation patterns calculated from the crystal structures of **Cu-Mepyz** and **Cu-py**, respectively.

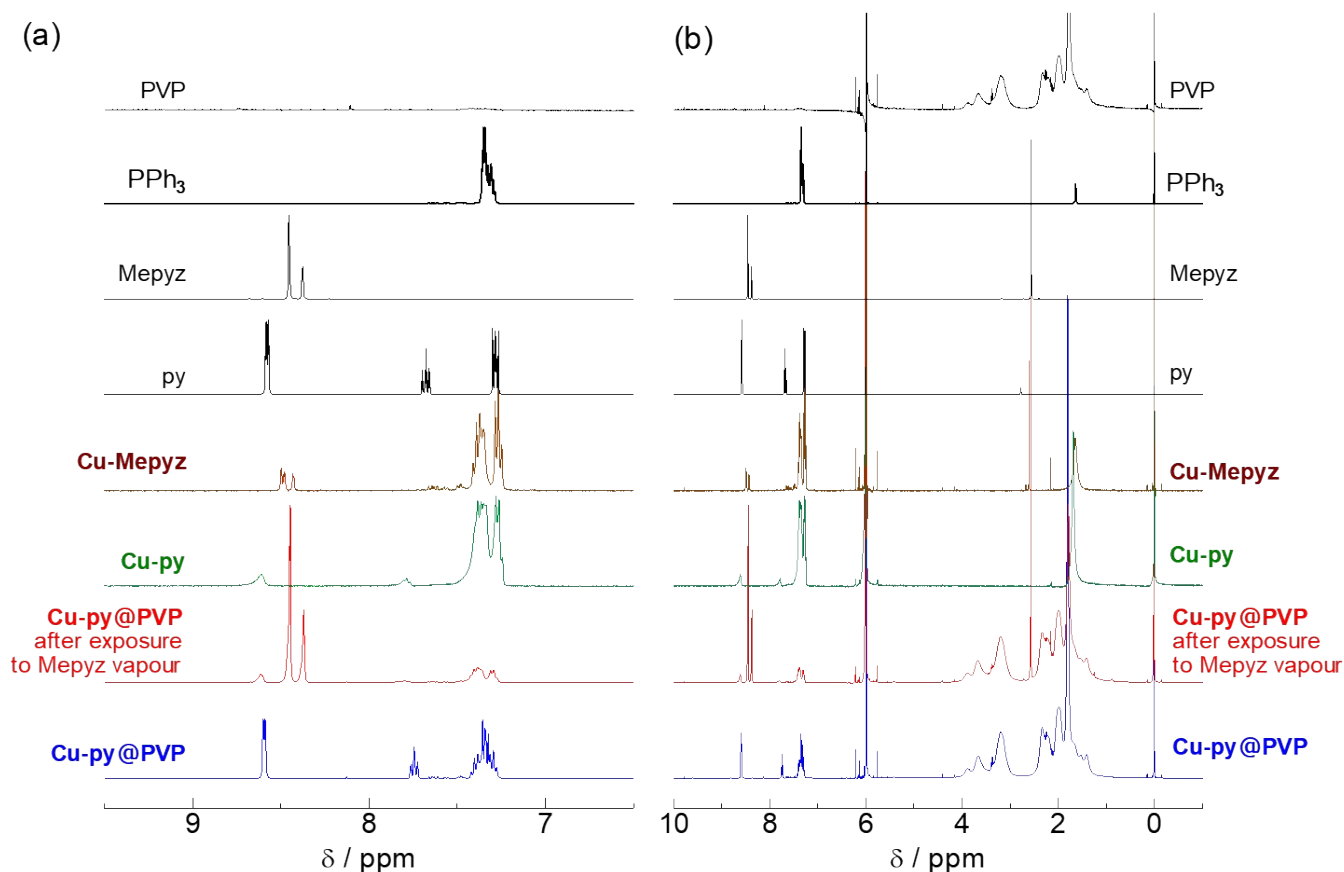


**Fig. S8** Changes of  $^1\text{H}$  NMR spectrum in (a) aromatic region and (b) whole range of **Cu-py@PVP** before (blue) and after (red) exposure to Mepyz vapour (293 K, 400 MHz, in  $\text{C}_2\text{D}_2\text{Cl}_4$ ). The spectral measurements were done for the solutions obtained by dissolving the film samples in  $\text{C}_2\text{D}_2\text{Cl}_4$ . The top five lines are the spectra of PVP polymer,  $\text{PPh}_3$ , Mepyz, py, **Cu-Mepyz**, and **Cu-py** in  $\text{C}_2\text{D}_2\text{Cl}_4$ .

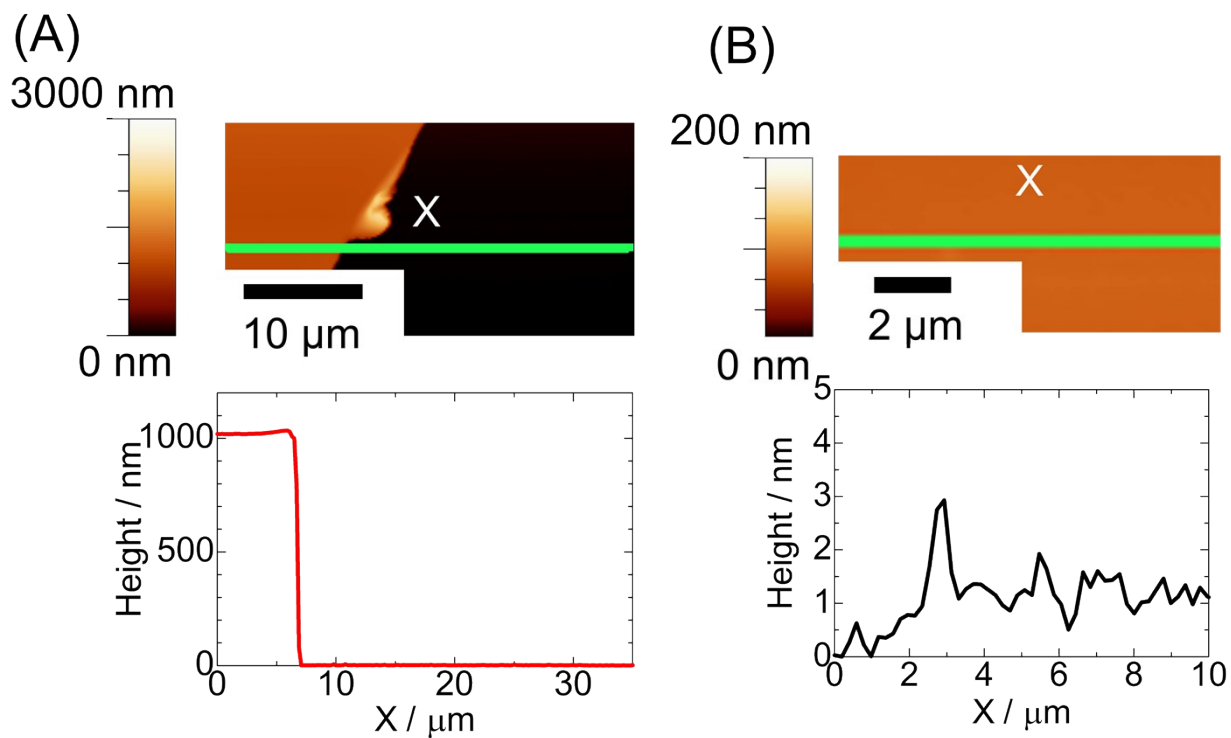


**Fig. S9** AFM images (top) and the height profile (bottom) of the surface of (A) the boundary area scratched **Cu-py@PVP** after exposure to Mepyz vapour and (B) Enlarged surface of **Cu-py@PVP** after exposure to Mepyz vapour.

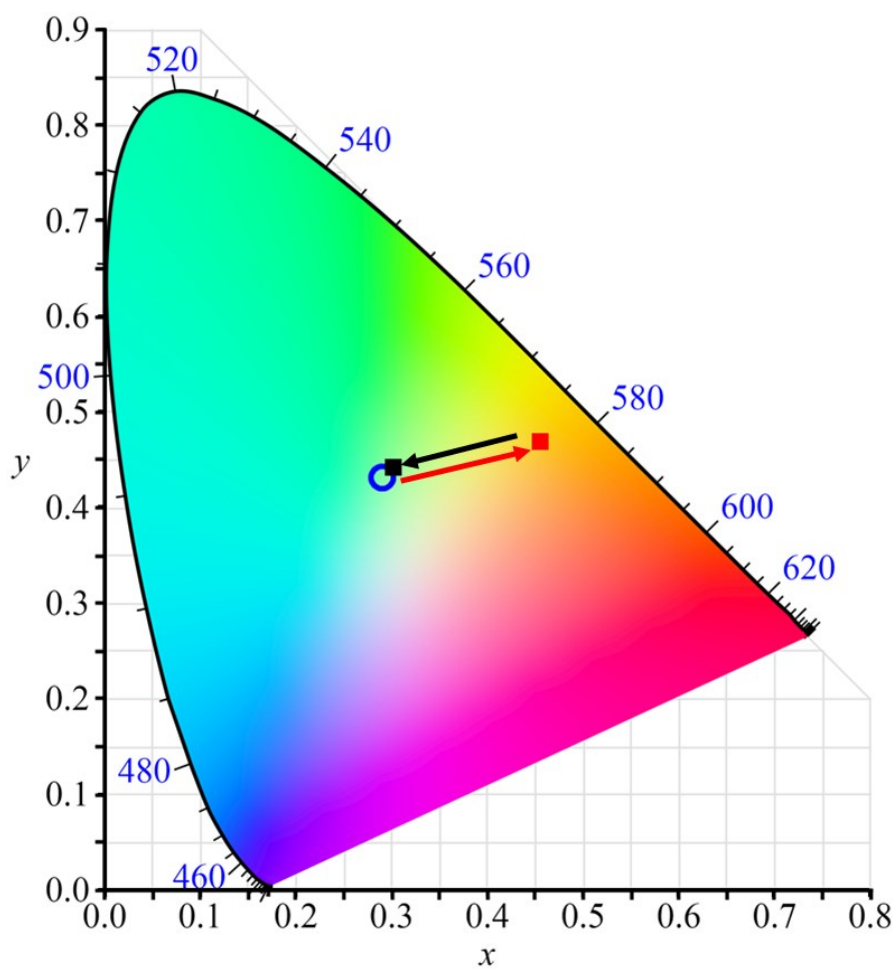


**Fig. S10** Change of Chromaticity color coordinate plots for **Cu-py@PVP** (blue circle) after exposure to Mepyz vapour (red square) and the subsequent exposure to py vapour (black square).

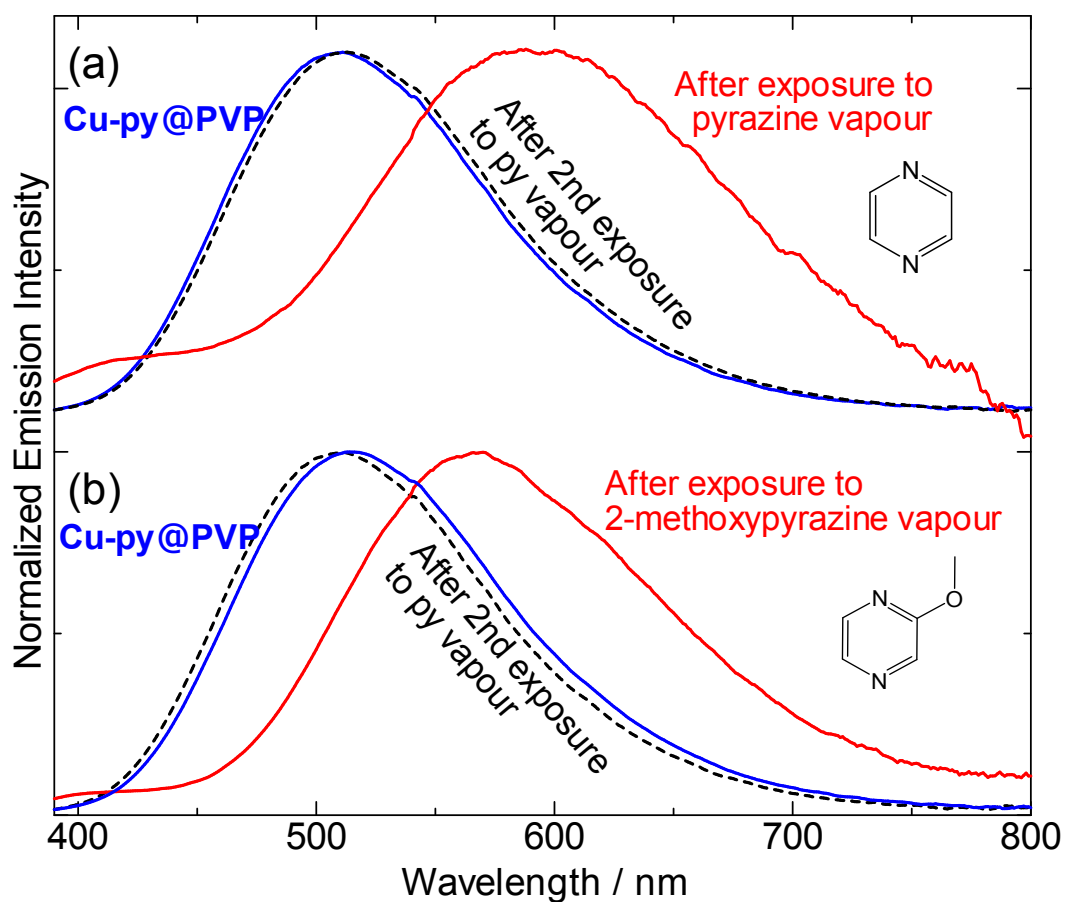


**Fig. S11** Changes of emission spectra of **Cu-py@PVP** (blue lines) before and (red lines) after exposure to (a) pyrazine and (b) 2-methoxypyrazine vapour for 2 min (298 K,  $\lambda_{\text{ex}} = 350$  nm). Black dotted lines are the spectra of the films after the subsequent exposure to py vapour for 2 min to recover the original **Cu-py@PVP**.

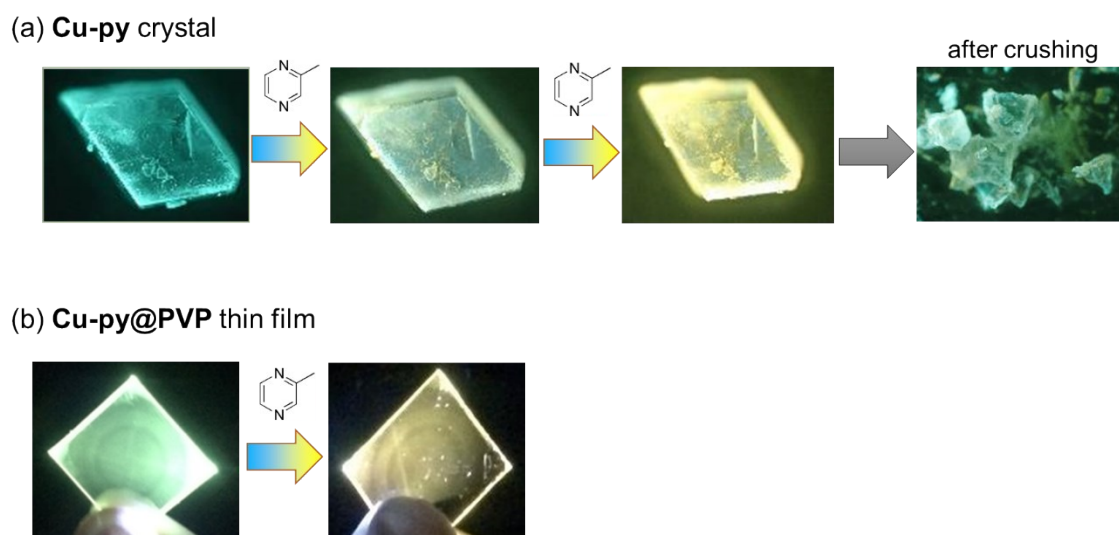


**Fig. S12** Photographs showing the luminescence changes for (a) **Cu-py** crystal and (b) **Cu-py@PVP** under exposure to Mepyz vapour. The right-side image in (a) is the photograph of crushed crystals after exposure to Mepyz vapour.

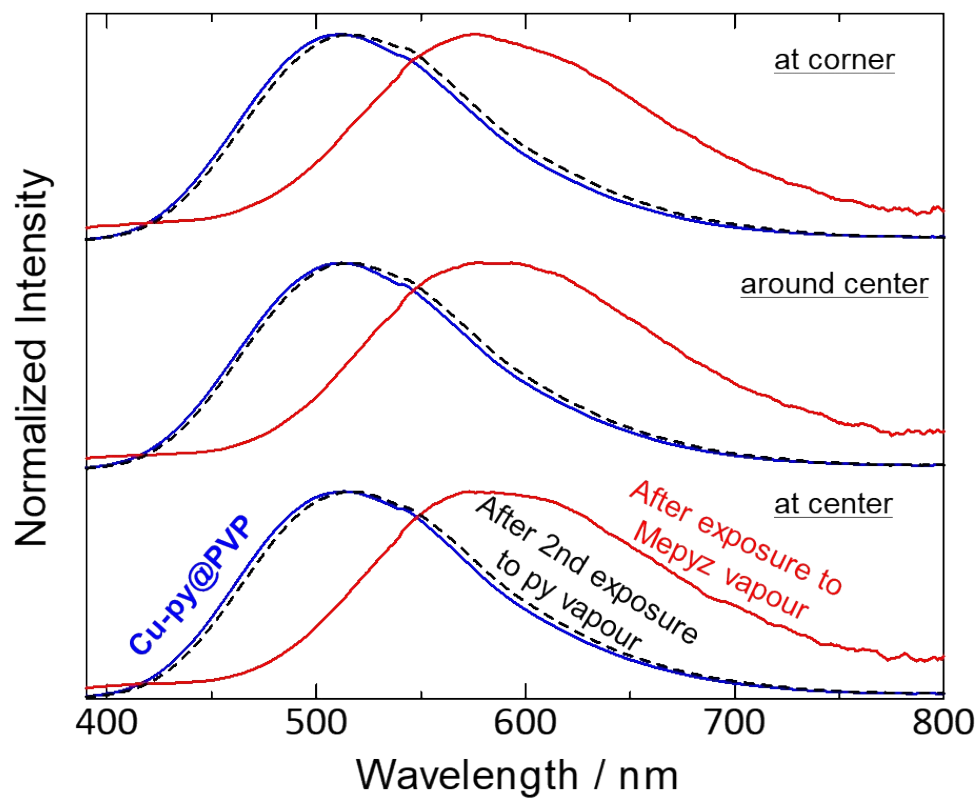


**Fig. S13** Changes of emission spectra ( $\lambda_{\text{ex}} = 350 \text{ nm}$ ) at several different positions on **Cu-py@PVP** (blue lines) after exposure to MepyZ vapour (red line) and the subsequent exposure to py vapour (black dash line).

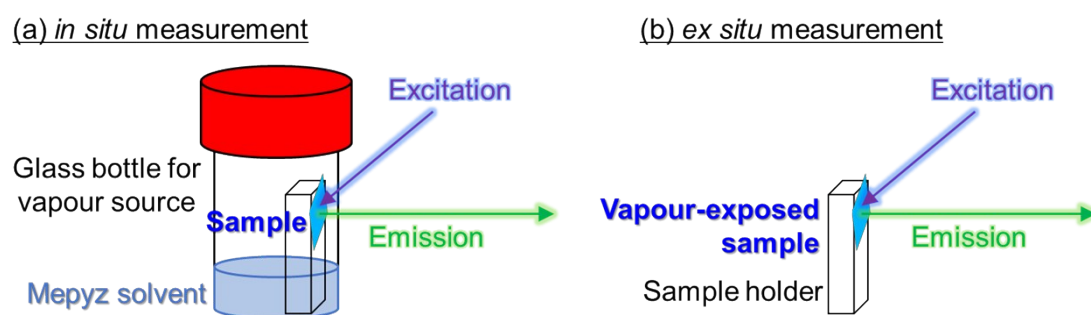


**Fig. S14** Schematic images of the experimental setup for (a) *in-situ* emission spectral measurement under vapour exposure and (b) *ex-situ* measurement for the vapour-exposed sample.



**Table S1** Crystal parameters and refinement data of **Cu-Mepyz** compared with **Cu-py**.

Complex	Cu-Mepyz	Cu-py
<i>T</i> / K	150	150
Formula	C <sub>41</sub> H <sub>36</sub> CuIN <sub>2</sub> P <sub>2</sub>	C <sub>41</sub> H <sub>35</sub> CuINP <sub>2</sub>
Formula weight	809.10	794.08
Crystal system	<i>monoclinic</i>	<i>triclinic</i>
Space group	<i>P2<sub>1</sub>/c</i>	<i>P-1</i>
<i>a</i> / Å	9.7754(1)	9.8484(2)
<i>b</i> / Å	37.378(3)	10.4600(2)
<i>c</i> / Å	10.999(1)	19.4312(4)
<i>α</i> / °	90	82.078(1)
<i>β</i> / °	115.013(1)	85.532(2)
<i>γ</i> / °	90	63.583(2)
<i>V</i> / Å <sup>3</sup>	3642.08(6)	1775.26(7)
<i>Z</i>	4	2
D <sub>cal</sub> / g cm <sup>-3</sup>	1.476	1.486
Reflections collected	20824	19616
Unique reflections	15531	13802
<i>R</i> <sub>int</sub>	0.0255	0.0250
GOF	1.046	1.151
<i>R</i> <sub>1</sub> ( <i>I</i> > 2σ( <i>I</i> )) <sup>a</sup>	0.0256	0.0308
<i>wR</i> <sub>2</sub> <sup>b</sup>	0.0683	0.1292

<sup>a</sup> $R_1 = \sum ||F_o| - |F_c|| / \sum |F_o|$ . <sup>b</sup>  $wR_2 = [\sum w(F_o^2 - F_c^2) / \sum w(F_o^2)]^{1/2}$ ,  $w = [\sigma_c^2(F_o^2) + (xP)^2 + yP]^{-1}$ ,  $P = (F_o^2 - 2F_c^2) / 3$ .

**Table S2** Selected bond lengths (Å) and angles (°) of **Cu-Mepyz** compared with **Cu-py**.

	<b>Cu-Mepyz</b>	<b>Cu-py</b>
Cu1-I1	2.625(3)	2.636(4)
Cu1-P1	2.274(1)	2.273(7)
Cu1-P2	2.278(2)	2.279(7)
Cu1-N1	2.107(2)	2.124(4)
I1-Cu1-P1	103.0(2)	102.8(2)
I1-Cu1-P2	113.0(2)	108.8(2)
I1-Cu1-N1	103.0(5)	108.7(8)
P1-Cu1-P2	125.0(3)	126.0(3)